

# We are IntechOpen, the world's leading publisher of Open Access books Built by scientists, for scientists

4,800

Open access books available

122,000

International authors and editors

135M

Downloads

Our authors are among the

154

Countries delivered to

TOP 1%

most cited scientists

12.2%

Contributors from top 500 universities



WEB OF SCIENCE™

Selection of our books indexed in the Book Citation Index  
in Web of Science™ Core Collection (BKCI)

Interested in publishing with us?  
Contact [book.department@intechopen.com](mailto:book.department@intechopen.com)

Numbers displayed above are based on latest data collected.  
For more information visit [www.intechopen.com](http://www.intechopen.com)



# Heat Transfer and Thermal Radiation at a General Three-Dimensional in a Nanofluid through a Porous Medium

*Gamal M. Abdel-Rahman and Faiza M.N. El-fayez*

## Abstract

In this chapter, the magnetohydrodynamic effects on heat transfer and thermal radiation at a stagnation point flowing in a nanofluid containing different types of nanoparticles namely, copper (Cu), alumina ( $Al_2O_3$ ) and titania ( $TiO_2$ ) through a porous medium have been investigated numerically. By using appropriate transformation for velocity and temperature into a set of non-linear coupled ordinary differential equations which are solved numerically. Numerical results are presented for velocity and temperature profiles for different parameters of the problem. Also, the effects of the pertinent parameters on the skin friction and the heat fluxes are obtained and discussed numerically and illustrated graphically.

**Keywords:** nanofluid, MHD, porous medium, thermal radiation, heat transfer

## 1. Introduction

Nanofluids have novel properties that make them potentially useful in many applications. They exhibit enhanced thermal conductivity and the convective heat transfer coefficient compared to the base fluid [1], so the nanofluids transfer heat at a higher rate than ordinary fluids (for example, water) which allows for more efficient heating or cooling while reducing energy consumption. Since nanofluid consists of very small sized solid particles, therefore in low solid concentration it is reasonable to consider nanofluid as a single-phase flow [2].

The term “nanofluid” refers to a liquid containing a suspension of submicronic solid particles (nanoparticles). This interest is generated by a variety of applications, ranging from laser-assisted drug delivery to electronic chip cooling. The term was coined by Choi [3]. The characteristic feature of nanofluids is thermal conductivity enhancement, a phenomenon observed by Masuda et al. [4]. This phenomenon suggests the possibility of using nanofluids in advanced nuclear system [5].

In recent years, numerous investigations have been conducted on the magnetohydrodynamic (MHD) flows and heat transfer because of its important applications in metallurgical industry, such as the cooling of continuous strips and filaments, drawn through a quiescent fluid and the purification of molten metals from non-metallic inclusions. It is known that the properties of the final product depend considerably on the rate of cooling during the manufacturing processes. The rate of cooling can be

controlled by drawing the strips in an electrically conducting fluid subject to a magnetic field, so that a final product of desired characteristics can be achieved [6]. One can solve this problem by using solid particles as an additive suspended into the base fluid as Choi [3] did, who first utilized and used fluids suspended by nanometer-sized solid particles. The resulting mixture referred to as a nanofluid possesses a substantially larger thermal conductivity compared to that of the traditional fluids [7]. These suspended nanoparticles can change the transport and thermal properties of the base fluid [8]. Therefore, by mixing the nanoparticles in the fluid, thermal conductivity of the fluid increases and the heat transfer capability improves.

The flow and heat transfer characteristics at a stagnation point, for both two-dimensional and axisymmetric, have been studied extensively in the literature [9]. These studies have been motivated by the fundamental nature of the boundary layer flows near such points by the exact applicability of similar solutions and by their relevance to the leading edge and nose regions of bodies in high speed flows. These two cases of two-dimensional and axisymmetric flows can be recognized as special cases of more general stagnation point flows. Both two-dimensional and axisymmetric flows were extended to three-dimensional by Howarth [10]. Bhattacharyya and Gupta [11] studied the flow and heat transfer in an incompressible viscous and electrically conducting fluid near a three-dimensional stagnation point of a body permeated by a uniform magnetic field. Analysis of such flows is very important in both theory and in practice. From a theoretical point of view, flows of this type are fundamental in fluid mechanics and forced convective heat transfer. On the other hand, from a practical point of view, these flows have applications in many manufacturing processes in industry such as the boundary layer along material handling conveyers, the aerodynamic extrusion of plastic sheet and petrochemical industries.

It is worth mentioning that the nanofluid model proposed by Buongiorno [12] was very recently used by Nield and Kuznetsov [13], Kuznetsov and Nield [14] and Bachok et al. [15] in their papers. Different from the above model.

The aim of the present chapter is to study the Magnetohydrodynamic effects on heat transfer and thermal radiation in an incompressible viscous fluid near the three-dimensional stagnation point of a body that is placed in a water based nanofluid through a porous medium containing different types of nanoparticles: copper (Cu), alumina ( $\text{Al}_2\text{O}_3$ ) and titania ( $\text{TiO}_2$ ). Numerical results are presented for velocity and temperature profiles for different parameters of the problem.

## 2. Mathematical analysis

Consider a flow of an electrically conducting fluid with heat transfer flow at a stagnation point of an incompressible viscous fluid past a body that is placed in a nanofluid of ambient uniform temperature  $T_\infty$  through a porous medium in the presence of radiation has been considered, where the body surface is kept at a constant temperature  $T_w$ . The stagnation point is located at the origin  $o$  of the Cartesian coordinate system  $oxyz$ . It was shown by Howarth [10] that the inviscid irrotational flow near  $o$  has the velocity components

$$u_e(x) = ax, \quad v_e(y) = by \quad (1)$$

with the constants  $a > 0$  and  $b \geq 0$  or  $b \leq 0$ .

The MHD body forces  $\bar{J} \times \bar{B}$  the Maxwell's equations:

$$\text{div} \bar{B} = 0, \quad \text{Curl} \bar{B} = \mu_m \bar{J} \quad \text{and} \quad \text{div} \bar{E} = 0$$

where  $\bar{J}$  is the electric current density,  $\bar{B} = B + d$  is the total magnetic field,  $\mu_f$  is the magnetic permeability and  $d$  is the induced magnetic field. The magnetic Reynolds number of the flow is taken to be small, so that the flow induction distortion of the applied magnetic field can be neglected as in the case with most of conducting fluids. The magnetic body force  $\bar{J} \times \bar{B}$  takes the form  $\sigma(\bar{V} \times \bar{B}) \times \bar{B}$ , therefore,  $\sigma(\bar{V} \times \bar{B}) \times \bar{B} = -\sigma B^2 \bar{V}$ , where  $\bar{V}$  is velocity vector  $\bar{V} = (u, v, w)$  and  $\bar{B} = (0, 0, B)$ . The Lorentz force (MHD body force) has two components:

$$F_x = -\sigma B^2 u, F_y = -\sigma B^2 v.$$

We now make the standard boundary-layer approximation, based on a scale analysis, and write the governing equations (see [6, 11]):

$$\frac{\partial u}{\partial x} + \frac{\partial v}{\partial y} + \frac{\partial w}{\partial z} = 0, \quad (2)$$

$$u \frac{\partial u}{\partial x} + v \frac{\partial u}{\partial y} + w \frac{\partial u}{\partial z} = a^2 x + \frac{\mu_{nf}}{\rho_{nf}} \frac{\partial^2 u}{\partial z^2} - \frac{\sigma B^2}{\rho_{nf}} u - \frac{\mu_{nf}}{\rho_{nf} K} u, \quad (3)$$

$$u \frac{\partial v}{\partial x} + v \frac{\partial v}{\partial y} + w \frac{\partial v}{\partial z} = b^2 x + \frac{\mu_{nf}}{\rho_{nf}} \frac{\partial^2 v}{\partial z^2} - \frac{\sigma B^2}{\rho_{nf}} v - \frac{\mu_{nf}}{\rho_{nf} K} v, \quad (4)$$

$$u \frac{\partial T}{\partial x} + v \frac{\partial T}{\partial y} + w \frac{\partial T}{\partial z} = \alpha_{nf} \frac{\partial^2 T}{\partial z^2} - \frac{1}{(\rho c)_{nf}} \frac{\partial q_r}{\partial z}, \quad (5)$$

Subject to the boundary conditions

$$\begin{aligned} u = v = w = 0, \quad T = T_w \quad \text{at } z = 0 \\ u \rightarrow u_e(x), \quad v \rightarrow v_e(y), \quad T \rightarrow T_\infty \quad \text{as } z \rightarrow \infty \end{aligned} \quad (6)$$

Here  $\mu_{nf}$  the viscosity of the nanofluid,  $\alpha_{nf}$  the thermal diffusivity of the nanofluid and  $\rho_{nf}$  the density of the nanofluid, which are given by

$$\begin{aligned} \mu_{nf} &= \frac{\mu_f}{(1-\varphi)^{5/2}}, \quad \alpha_{nf} = \frac{k_{nf}}{(\rho C_p)_{nf}}, \quad \rho_{nf} = (1-\varphi)\rho_f + \varphi\rho_s, \\ (\rho C_p)_{nf} &= (1-\varphi)(\rho C_p)_f + \varphi(\rho C_p)_s, \\ \frac{k_{nf}}{k_f} &= \frac{(k_s + 2k_f) - 2\varphi(k_f - k_s)}{(k_s + 2k_f) + \varphi(k_f - k_s)} \end{aligned} \quad (7)$$

where  $q_r$  is the energy flux which is relative to a frame moving with the nanofluid velocity. Using the Rosseland approximation (Rashed [16]), the radiative heat flux  $q_r$  could be expressed by

$$q_r = -k_1 \frac{\partial T^4}{\partial z} \quad (8)$$

where  $k_1 = 4\sigma^*/3k^*$  is the nanofluid thermal conductivity.

Assuming that the temperature difference within the flow is sufficiently small such that  $T^4$  could be approached as the linear function of temperature;

$$T^4 \cong 4T_\infty^3 T - 3T_\infty^4 \quad (9)$$

Further, we look for a solution of Eqs. (2)–(5) of the form

$$\begin{aligned} u &= axf'(\eta), \quad v = byg'(\eta), \quad w = -\sqrt{av_f}(f + cg), \\ \theta(\eta) &= \frac{(T - T_\infty)}{(T_w - T_\infty)}, \quad \eta = \sqrt{a/\nu_f}z \end{aligned} \quad (10)$$

where  $c = b/a$  is the ratio of the gradient of velocities in the  $y$ - and  $x$ -directions, and primes denote differentiation with respect to  $z$ . Substituting Eqs. (8)–(10) in Eqs. (2)–(5), we obtain the following nonlinear ordinary differential equations:

$$\left( \frac{1}{(1 - \varphi)^{5/2} \left( 1 - \varphi \left( 1 - \rho_s/\rho_f \right) \right)} \right) \left[ f'''' - M(1 - \varphi)^{5/2} f' - S f' \right] + (f + cg) f'' - f'^2 + 1 = 0, \quad (11)$$

$$\left( \frac{1}{(1 - \varphi)^{5/2} \left( 1 - \varphi \left( 1 - \rho_s/\rho_f \right) \right)} \right) \left[ g'''' - M(1 - \varphi)^{5/2} g' - S g' \right] + (f + cg) g'' + c(1 - g'^2) = 0, \quad (12)$$

$$\left( \frac{((k_{nf}/k_f) + Q)}{Pr \left( 1 - \varphi \left( 1 - \left( (\rho C_p)_s / (\rho C_p)_f \right) \right) \right)} \right) \theta'' + (f + cg) \theta' = 0, \quad (13)$$

With the appropriate boundary conditions:

$$\begin{aligned} f'(0) &= 0, \quad g'(0) = 0, \quad f(0) = -c g(0), \quad \theta(0) = 1, \\ f'(\infty) &= 1, \quad g'(\infty) = 1, \quad \theta(\infty) = 0. \end{aligned} \quad (14)$$

where the prime denotes a partial differentiation with respect to  $\eta$ ,  $M = \sigma B^2/a\rho_f$  is the Magnetic field parameter,  $S = \nu_f/a\kappa$  is the Porous medium parameter and  $Q = 4k_1T_\infty^3$  is the Thermal radiation parameter.

There is no loss of generality in the requirement that  $|a| \geq |b|$  with  $a > 0$ . Clearly  $b = 0$  corresponds to the plane stagnation point flow case, while  $b = a$  is the axisymmetric case. The case  $0 < c < 1$  displays the nodal stagnation point of attachment ( $b > 0$ ), while  $-1 < c < 0$  displays the saddle points of attachment ( $b < 0$ ) [5].

### 3. Skin-friction coefficient and Nusselt number

The parameters of engineering interest for the present problem are the local skin-friction coefficients  $C_{fx}$  and  $C_{fy}$ , along the  $x$ - and  $y$ -directions, respectively, and the local Nusselt number  $Nu_x$ , which are defined as

$$C_{fx} = \frac{\tau_{wx}}{ax\rho_f u_w^2}, \quad C_{fy} = \frac{\tau_{wy}}{by\rho_f u_w^2}, \quad Nu_x = \frac{u_w^2 q_w}{ak_f(T_w - T_\infty)} \quad (15)$$

where  $\tau_{wx}$  and  $\tau_{wy}$  are the surface shear stresses along the  $x$ - and  $y$ -directions, respectively, and  $q_w$  is the surface heat flux, which are given by

$$\tau_{wx} = \mu_{nf} \left( \frac{\partial u}{\partial z} \right)_{z=0}, \quad \tau_{wy} = \mu_{nf} \left( \frac{\partial v}{\partial z} \right)_{z=0}, \quad q_w = -k_{nf} \left( \frac{\partial T}{\partial z} \right)_{z=0} \quad (16)$$

Using Eqs. (10), (15), and (16), we obtain

$$\begin{aligned} \text{Re}_x^{1/2} C_{fx} &= \frac{1}{(1-\varphi)^{5/2}} f''(0), & \text{Re}_x^{1/2} C_{fy} &= \frac{1}{(1-\varphi)^{5/2}} g''(0) \\ \text{Re}_x^{-1/2} \text{Nu}_x &= -\frac{k_{nf}}{k_f} \theta'(0) \end{aligned} \quad (17)$$

where  $\text{Re}_x = u_w^4 / \nu_f$  is the local Reynolds number.

## 4. Results and discussion

Numerical solutions to the nonlinear ordinary differential Eqs. (11)–(14) were obtained using the modified fourth order Runge-Kutta method along with Nachtsheim-Swigert shooting technique [17]. In order to gain physical insight, the velocity and the temperature profiles have been discussed by assigning numerical values to the parameter, encountered in the problem which the numerical results are tabulated and displayed with the graphical illustrations **Figure 1**. We find the missing slopes  $f''(0)$ ,  $g''(0)$  and  $-\theta'(0)$  for some values of the governing parameters, namely the nanoparticle volume fraction  $\varphi$  and the ratio of the gradient of velocities in the  $i$ - and  $x$ -directions  $c$ , where  $0 < c < 1$  displays the nodal stagnation point of attachment and  $-1 < c < 0$  displays the saddle points of attachment. Three types of nanoparticles were considered, namely, copper (Cu), alumina ( $\text{Al}_2\text{O}_3$ ) and titania ( $\text{TiO}_2$ ). Following Oztop and Abu-Nada [18], the value of the Prandtl number  $P_r$  is taken as 6.2 (for water) and the volume fraction of nanoparticles is from 0 to 0.2 ( $0 \leq \varphi \leq 0.2$ ) in which  $\varphi$  corresponds to the regular Newtonian fluid. The numerical results are summarized in **Figures 2–6**. It is worth mentioning that we have used data related to the thermophysical properties of the fluid and nanoparticles as listed in **Table 1** [18] to compute each case of the nanofluid.

**Figures 2, 3** and **5a–c**, display the velocity  $f'(\eta)$ ,  $g'(\eta)$  and the temperature  $\theta(\eta)$  profiles under the different parameters of the problem as magnetic field parameter, porous medium parameter and nanoparticle parameter. It is observed that the velocity profile decreases, while the temperature profile increases with the increase in each of magnetic field parameter, porous medium parameter and nanoparticle parameter.

The effects of the nanoparticle volume fractions on the velocity and the temperature profiles are shown in **Figure 4a–c**, respectively. It is observed that the

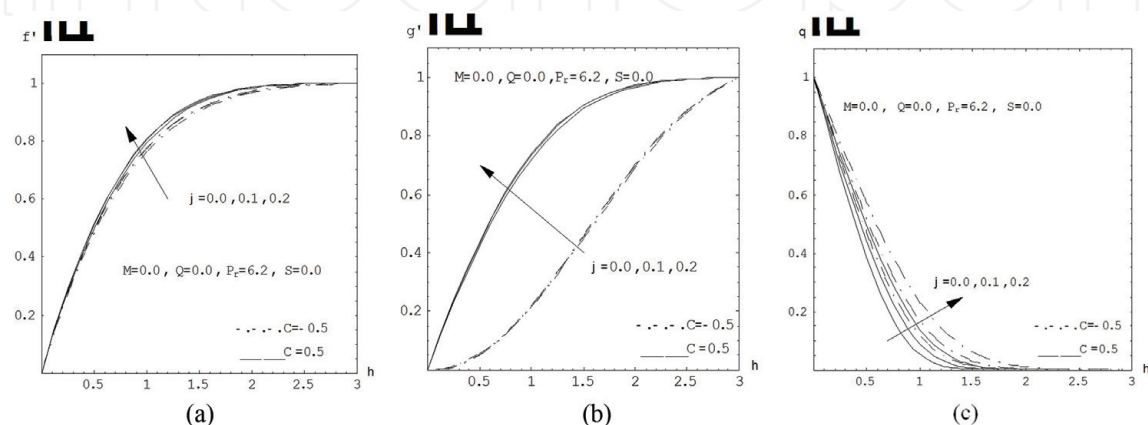


**Figure 1.** Effect of nanoparticle volume fractions on (a) the velocity profile  $f'(\eta)$ , (b) the velocity profile  $g'(\eta)$  and (c) the temperature profile  $\theta(\eta)$  at  $c = 0.5$  and  $-0.5$  for copper-water nanofluid.

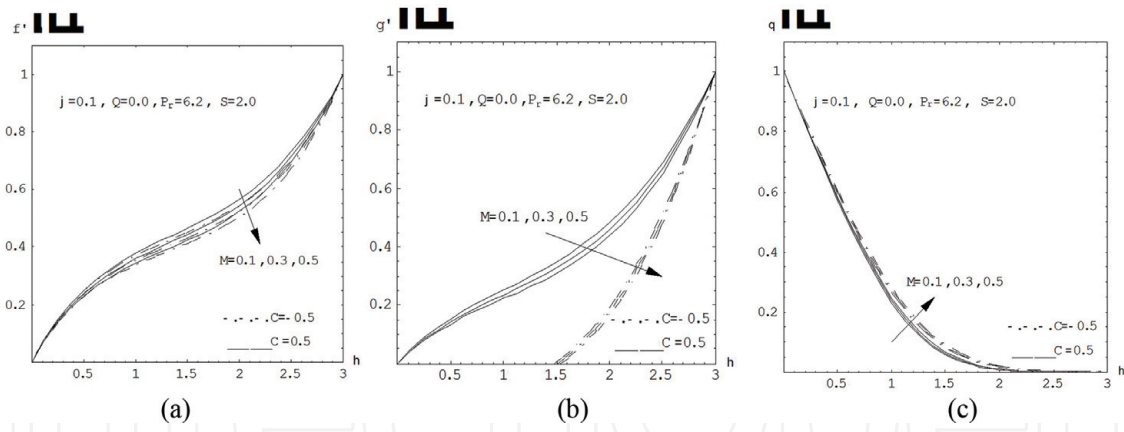


**Figure 2.** Effect of magnetic field parameter on (a) the velocity profile  $f'(\eta)$ , (b) the velocity profile  $g'(\eta)$  and (c) the temperature profile  $\theta(\eta)$ .

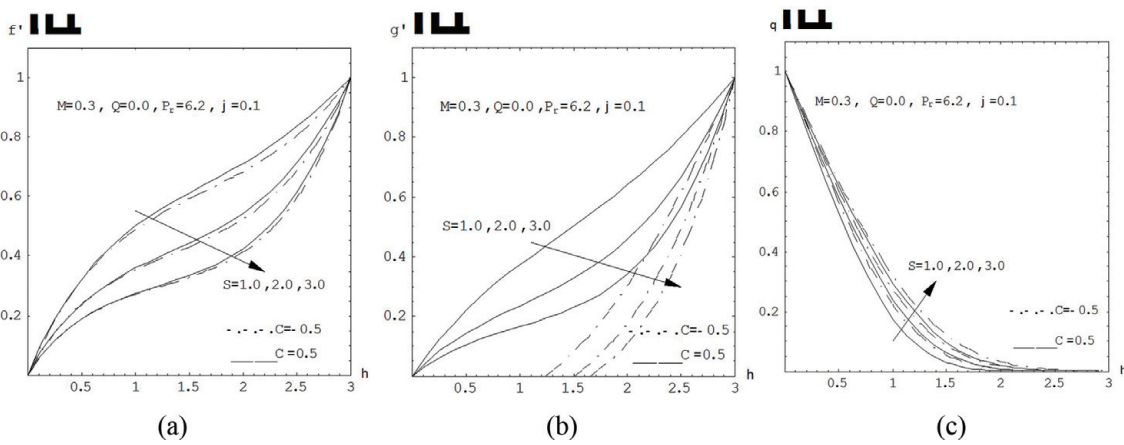


**Figure 3.** Effect of porous medium parameter on (a) the velocity profile  $f'(\eta)$ , (b) the velocity profile  $g'(\eta)$  and (c) the temperature profile  $\theta(\eta)$ .

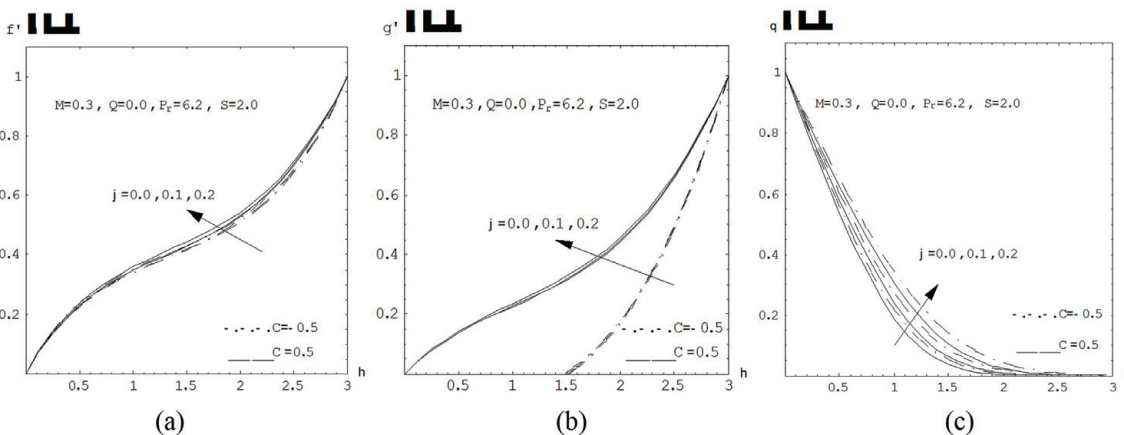


**Figure 4.** Effect of nanoparticle volume fractions on (a) the velocity profile  $f'(\eta)$ , (b) the velocity profile  $g'(\eta)$  and (c) the temperature profile  $\theta(\eta)$ .

velocity and the temperature profiles increase with the increase of the nanoparticle volume fractions. The effects of thermal radiation parameter on the temperature profile are shown in **Figure 6**; also, we found that the temperature profiles increase with the increase of thermal radiation parameters. i.e. as expected, since the effect of thermal radiation is to decrease the rate of energy transport to the fluid.

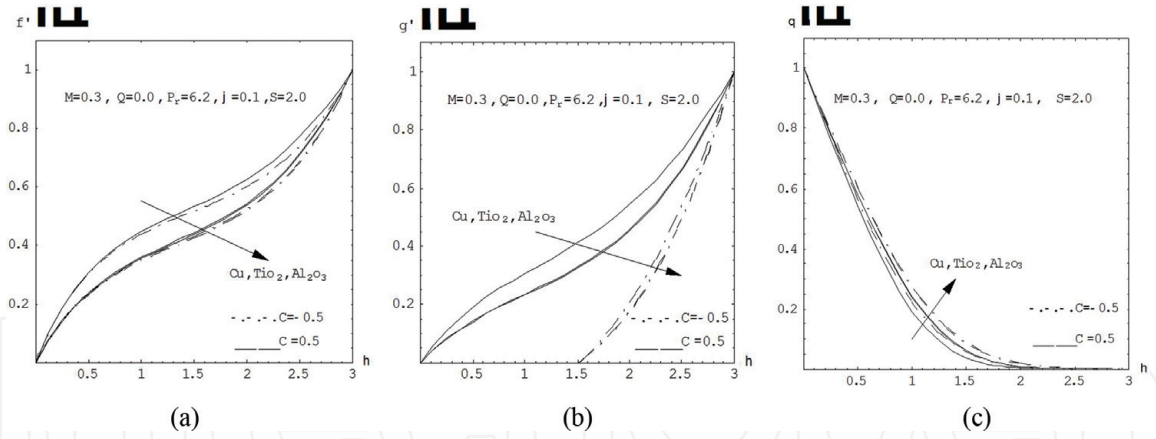


**Figure 5.**  
 Effect of nanoparticle on (a) the velocity profile  $f'(\eta)$ , (b) the velocity profile  $g'(\eta)$  and (c) the temperature profile  $\theta(\eta)$ .

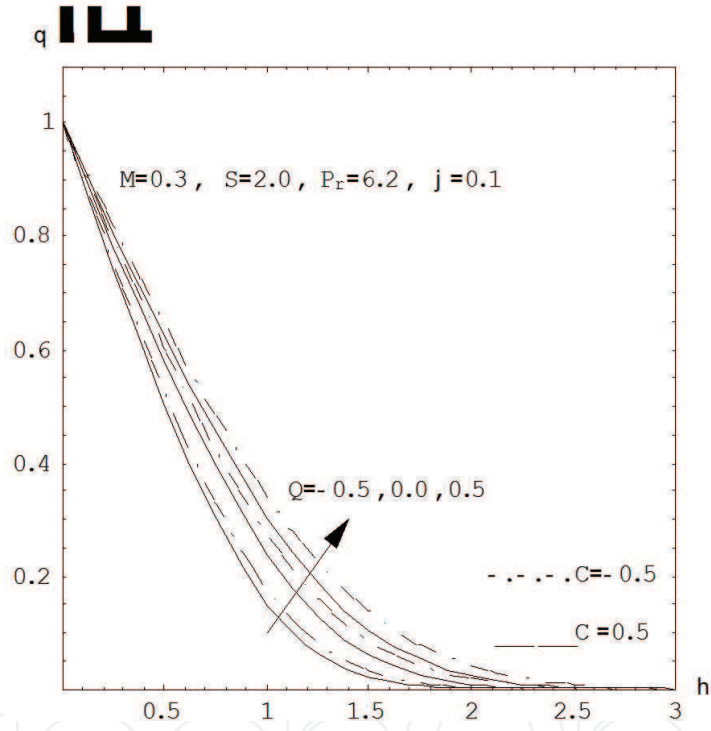


**Figure 6.**  
 Effect of the thermal radiation parameter on the temperature profile  $\theta(\eta)$ .

Physical properties	Fluid phase (water)	Cu	Al <sub>2</sub> O <sub>3</sub>	TiO <sub>2</sub>
$C_p$ (J / kg K)	4179	385	765	686.2
$\rho$ (kg / m <sup>3</sup> )	997.1	8933	3970	4250
$k$ (W / mK)	0.613	400	40	8.9538
$\alpha \times 10^7$ (m <sup>2</sup> / s)	1.47	1163.1	131.7	30.7

**Table 1.**  
 Thermophysical properties of fluid and nanoparticles [18].



$M$	$S$	$\varphi$	$Q$	$Re_x^{1/2} C_{fx}$		$Re_x^{1/2} C_{fy}$		$Re_x^{-1/2} Nu_x$	
				$c = -0.5$	$c = 0.5$	$c = -0.5$	$c = 0.5$	$c = -0.5$	$c = 0.5$
0.1	2.0	0.1	0.0	0.905057	0.912069	-0.359099	0.524052	1.08178	1.14672
				0.87735	0.883391	-0.356488	0.501349	1.06709	1.12757
				0.85163	0.856843	-0.353334	0.480884	1.05291	1.10938
0.3	1.0	0.1	0.0	1.10357	1.11976	-0.352305	0.706599	1.17147	1.27281
				0.87735	0.88339	-0.356488	0.501349	1.06709	1.12757
				0.73820	0.74059	-0.358357	0.397432	0.98337	1.02393
0.3	2.0	0.0	0.0	0.654066	0.658315	-0.267656	0.371336	1.18524	1.2446
				0.87735	0.88339	-0.356488	0.501349	1.06709	1.26757
				1.11575	1.12365	-0.444151	0.638333	1.01473	1.29428
0.3	2.0	0.1	-0.5					1.28272	1.34486
								1.06709	1.12757
								0.94130	1.00087

**Table 2.**

Numerical of the values skin-friction coefficient ( $Re_x^{1/2}C_{fx}$ ) and ( $Re_x^{1/2}C_{fy}$ ) along  $x$ - and  $y$ -directions and the local Nusselt number ( $Re_x^{-1/2}Nu_x$ ) with  $M, S, \varphi$  and  $Q$ , when  $Pr = 6.2$ .

From **Table 2**, the numerical values of the skin-friction and the local Nusselt number are given in **Table 2**. For an increase in the magnetic field parameter  $M$ , we observe that the skin-friction coefficient along  $x$ - and  $y$ -directions and the local Nusselt number decrease when  $c = 0.5$ , but at  $c = -0.5$ , the skin-friction coefficient along  $x$ -direction and the local Nusselt number decrease, while the skin-friction coefficient along  $y$ -direction increases. While, with an increase in the porous medium parameter  $S$ , we observe that the skin-friction coefficient and the local Nusselt number decrease when  $c = -0.5$  and  $c = -0.5$ .

With an increase in nanoparticle volume fractions  $\varphi$ , we observe that the skin-friction coefficient increases and the local Nusselt number increases when  $c = 0.5$ , but at  $c = -0.5$ , the skin-friction coefficient along  $y$ -direction and the local Nusselt number decrease, while the skin-friction coefficient along  $x$ -direction increases. While, with an increase in the thermal radiation parameter  $Q$ , we observe that the local Nusselt number decreases when  $c = -0.5$  and  $c = -0.5$ .

## 5. Conclusions

In the present chapter, the magnetohydrodynamic effects on heat transfer and thermal radiation at a stagnation point flowing in a nanofluid containing different types of nanoparticles namely, copper (Cu), alumina ( $Al_2O_3$ ) and titania ( $TiO_2$ ) through a porous medium have been investigated numerically. By using appropriate transformation for velocity and temperature into a set of non-linear coupled ordinary differential equations which are solved numerically, the governing equations were:

1. With the increasing values of the magnetic field parameter, porous medium parameter and nanoparticle parameter, it is observed that the velocity profile decreases, while the temperature profile increases.

2. The velocity and the temperature profiles increase with the increase of the nanoparticle volume fractions.
3. For the effects of thermal radiation parameter on the temperature profile, we found that the temperature profiles increase with the increase of thermal radiation parameters
4. For an increase in the magnetic field parameter  $M$ , we observe that the skin-friction coefficient along  $x$ - and  $y$ -directions and the local Nusselt number decrease when  $c = 0.5$ , but at  $c = -0.5$ , the skin-friction coefficient along  $x$ -direction and the local Nusselt number decrease, while the skin-friction coefficient along  $y$ -direction increases.
5. About the effects of the porous medium parameter  $S$ , we observe that the skin-friction coefficient and the local Nusselt number decrease when  $c = -0.5$  and  $c = -0.5$ .
6. The local Nusselt number decreases when  $c = -0.5$  and  $c = -0.5$ , with the increase of the thermal radiation parameter  $Q$ .

## Nomenclature

$a$	constant
$B$	magnetic field
$b$	constant
$c$	the ratio of the gradient of velocities in the $y$ - and $x$ -directions
$C_{fx}, C_{fy}$	skin friction in the $y$ - and $x$ -directions
$d$	the induced magnetic field
$k_{nf}$	the thermal conductivity of the nanofluid
$k_f$	the thermal conductivities of the fluid
$k_s$	the thermal conductivities of the solid fractions
$k_1$	the nanofluid thermal conductivity
$k^*$	mean absorption coefficient
$Nu_x$	Nusselt number
$M$	magnetic field parameter
$Q$	thermal radiation parameter
$q_r$	the energy flux which is relative to a frame moving with the nanofluid velocity
$q_w$	the surface heat flux
$T$	temperature distribution
$T_w$	constant temperature
$T_\infty$	ambient uniform temperature
$S$	porous medium parameter
$Re_x$	the local Reynolds number
$u$	velocity in the $x$ -direction
$v$	velocity in the $y$ -direction
$w$	velocity in the $z$ -direction
$x$	horizontal distance
$y$	vertical distance
$z$	normal distance
Greek symbols	
$\alpha_{nf}$	the thermal diffusivity of the nanofluid

$\eta$	similarity variable
$\theta$	dimensionless temperature distribution
$\mu_f$	the viscosity of the fluid
$\mu_{nf}$	the viscosity of the nanofluid
$\rho_f$	the densities of the fluid
$\rho_s$	density of the solid fractions
$\rho_{nf}$	density of the nanofluid
$\nu_f$	kinematic viscosity of the fluid
$(\rho C_p)_{nf}$	the heat capacity of the nanofluid
$(\rho C_p)_f$	the heat capacity of the fluid
$(\rho C_p)_s$	the heat capacity of the solid fractions
$\kappa$	the permeability of the porous medium
$\sigma$	electrical conductivity
$\sigma^*$	Stephan-Boltzmann constant
$\tau_{wx}, \tau_{wy}$	the surface shear stresses along the $x$ - and $y$ -directions
$\varphi$	nanoparticle volume fraction
Subscripts	
$w, \infty$	conditions at the surface and in the free stream

## Author details


Gamal M. Abdel-Rahman<sup>1\*</sup> and Faiza M.N. El-fayez<sup>2</sup>

<sup>1</sup> Department of Mathematics, Faculty of Science, Benha University, Benha, Egypt

<sup>2</sup> Mathematical Science Department, College of Sciences, Princess Nourah bint Abdulrahman University, KSA

\*Address all correspondence to: gamalm60@yahoo.com

## IntechOpen

© 2018 The Author(s). Licensee IntechOpen. This chapter is distributed under the terms of the Creative Commons Attribution License (<http://creativecommons.org/licenses/by/3.0>), which permits unrestricted use, distribution, and reproduction in any medium, provided the original work is properly cited. 

## References

- [1] Kakaç S, Pramuanjaroenkij A. Review of convective heat transfer enhancement with nanofluids. *International Journal of Heat and Mass Transfer*. 2009;52:3187-3196
- [2] Xuan YM, Li Q. Heat transfer enhancement of nanofluid. *International Journal of Heat and Fluid Flow*. 2000;21:58-64
- [3] Choi S. Enhancing thermal conductivity of fluids with nanoparticle. In: Siginer DA, Wang HP, editors. *Developments and Applications of Non-Newtonian Flows*. ASME MD vol. 231 and FED vol. 66; 1995. pp. 99-105
- [4] Masuda H, Ebata A, Teramae K, Hishinuma N. Alteration of thermal conductivity and viscosity of liquid by dispersing ultra-fine particles. *Netsu Bussei*. 1993;7:227-233
- [5] Buongiorno J, Hu W. Nanofluid coolants for advanced nuclear power plants. In: Paper no. 5705, Proceedings of ICAPP'05; Seoul. May 2005. pp. 15-19
- [6] Vajravelu K, Hadjinicolaou A. Convective heat transfer in an electrically conducting fluid at a stretching surface with uniform free stream. *International Journal of Engineering Science*. 1997;35:1237-1244
- [7] Eastman JA, Choi SUS, Li S, Yu W, Thompson J. Anomalous increased effective thermal conductivities of ethylene glycol-based nanofluids containing copper nanoparticles. *Applied Physics Letters*. 2001;78(6): 718-720
- [8] Lotfi R, Saboohi Y, Rashidi AM. Numerical study of forced convective heat transfer of nanofluids: Comparison of different approaches. *International Communications in Heat and Mass Transfer*. 2010;74:37
- [9] Hiemenz K. Die Grenzschicht an einem in den gleichförmigen Flüssigkeitsstrom eingetauchten geraden Kreiszyylinder. *Dingler's Polytechnisches Journal*. 1911;326:321-410
- [10] Howarth L. The boundary layer in three dimensional flow—Part II. The flow near a stagnation point stagnation point. *Philosophical Magazine Series*. 1951;7(42):1433-1440
- [11] Bhattacharyya S, Gupta AS. MHD flow and heat transfer at a general three-dimensional at a stagnation point. *International Journal of Non-Linear Mechanics*. 1998;33:125-134
- [12] Buongiorno J. Convective transport in nanofluids. *ASME Journal of Heat Transfer*. 2006;128:240-250
- [13] Nield DA, Kuznetsov AV. Thermal instability in a porous medium layer saturated by a nanofluid. *International Journal of Heat and Mass Transfer*. 2009;52:5796-5801
- [14] Kuznetsov AV, Nield DA. Natural convective boundary-layer flow of a nanofluid past a vertical plate. *International Journal of Thermal Sciences*. 2010;49:243-247
- [15] Bachok N, Ishak A, Pop I. Boundary-layer flow of nanofluids over a moving surface in a flowing fluid. *International Journal of Thermal Sciences*. 2010; 49(9):1663-1668
- [16] Rashed GMA. Chemical entropy generation and MHD effects on the unsteady heat and fluid flow through a porous medium. *Journal of Applied Mathematics*. 2016;2016:9. Article ID 1748312
- [17] Adams JA, Rogers DF. *Computer-Aided Heat Transfer Analysis*. McGraw-Hill; 1973

[18] Oztop HF, Abu-Nada E. Numerical study of natural convection in partially heated rectangular enclosures filled with nanofluids. *International Journal of Heat and Fluid Flow*. 2008;**29**:1326-1336

IntechOpen

IntechOpen